Anisotropic Superfluidity in a Dipolar Bose Gas

Christopher Ticknor,[1] Ryan M. Wilson,[2] and John L. Bohn[2]

[1]*Theoretical Division, Los Alamos National Laboratory, Los Alamos, New Mexico 87545, USA*
[2]*JILA, NIST and Department of Physics, University of Colorado, Boulder, Colorado 80309, USA*

We study the superfluid character of a dipolar Bose-Einstein condensate (DBEC) in a quasi-two dimensional geometry. We consider the dipole polarization to have some nonzero projection into the plane of the condensate so that the effective interaction is anisotropic in this plane, yielding an anisotropic dispersion relation. By performing direct numerical simulations of a probe moving through the DBEC, we observe the sudden onset of drag or creation of vortex-antivortex pairs at critical velocities that depend strongly on the direction of the probe's motion. This anisotropy emerges because of the anisotropic manifestation of a rotonlike mode in the system.

A quintessential feature of a superfluid is its ability to support dissipationless flow. For example, a small probe can move through the a superfluid without experiencing a drag force, provided that it moves below a certain critical velocity. As Landau famously explained, when this critical velocity is exceeded, energy can be dissipated into collective excitations of the fluid, leading to a nonzero drag force on the probe [1]. In a dilute superfluid such as a Bose-Einstein condensate (BEC) of alkali atoms, these excitations are simply sound waves and the critical velocity is equal to the sound velocity. By contrast, for a strongly interacting superfluid such as liquid ^{4}He, the relevant excitations correspond to nontrivial many-body excitations, dubbed rotons. These modes lead to a superfluid critical velocity that is significantly less than the speed of sound. Moreover, they represent a vital link between a macroscopic observable such as superfluidity, and the detailed, microscopic physics of the fluid. This critical velocity has been verified experimentally via measurements of ion-drift velocity in the superfluid phase of ^{4}He [2].

Currently, a major research thrust is working to produce BECs composed of particles with dipolar interactions, using either strongly magnetic atoms [3] or dipolar molecules [4]. This fascinating new breed of superfluids can also exhibit rotonlike features in their spectra, despite existing in a dilute gaseous state [5]. By tuning either the dipole moment or the density of the constituents, the spectra of these gases can be widely varied [6]. The relation between superfluidity and elementary excitations can therefore be probed in these gases as never before. Moreover, these dipolar BECs (DBECs) bring something entirely new to the subject, namely, an anisotropic interaction that should generate an anisotropic critical velocity. It is this basic property of anisotropic superfluidity that we explore in this Letter.

We consider a DBEC in a quasi-two-dimensional (Q2D), or pancake-shaped trapping potential and allow the dipoles to be polarized at an arbitrary angle with respect to this plane. Numerical simulations of a probe moving through the DBEC reveal a sudden onset of drag

at a critical velocity that is quite different for different directions of the probe's motion. Specifically, the critical velocity is larger in the direction parallel to the dipoles' orientation than in the perpendicular direction. In spite of this anisotropy, the speed of sound, corresponding to long-wavelength excitations, remains isotropic. For sufficiently small probes, the drag is due to the excitation of the roton-like modes, whereas for larger probes it arises from the production of vortex-antivortex pairs, as observed in isotropic alkali-atom BECs [7,8]. Even in this case, however, the spinning off of vortices depends strongly on the direction of motion of the probe, so that the effects of anisotropy should be readily observable.

We work in a Q2D geometry by assuming that there is a strong one-dimensional (1D) harmonic trap in the z direction, $U_{1D}(z) = \frac{1}{2} m\omega_z^2 z^2$, where m is the bosonic mass and ω_z is the trapping frequency. This allows the condensate wave function to be written in the separable form $\Psi(\mathbf{r}, t) = \chi(z)\psi(\boldsymbol{\rho}, t)$ where $\chi(z)$ is the ground state harmonic oscillator wave function. By inserting this ansatz into the Gross-Pitaevskii equation (GPE), describing the dilute, zero-temperature DBEC, and integrating out the z dependence, we derive the modified, time-dependent GPE for the Q2D system,

$$i\hbar\partial_t\psi = \left\{-\frac{\hbar^2}{2m}\nabla^2 + V_p + g|\psi|^2 + g_d\Phi\right\}\psi, \quad (1)$$

where $\psi = \psi(\boldsymbol{\rho}, t)$ is the in-plane condensate wave function, $V_p = V_p(\boldsymbol{\rho}, t)$ is a time-dependent probe potential, $g = 2\sqrt{2\pi}\hbar^2 a_s/ml_z$ is the mean-field coupling for contact interactions, a_s is the scattering length, $l_z = \sqrt{\hbar/m\omega_z}$ is the axial harmonic oscillator length, $g_d = d^2/\sqrt{2\pi}l_z$ is the dipole-dipole interaction (DDI) coupling and $g_d\Phi = g_d\Phi(\boldsymbol{\rho}, t)$ is the mean-field potential due to the DDI, where $\Phi(\boldsymbol{\rho}, t) = \frac{4\pi}{3}\mathcal{F}^{-1}[\tilde{n}(\mathbf{k}, t)F(\frac{kl_z}{\sqrt{2}})]$, and $\mathcal{F}$ is the 2D Fourier transform operator and $\tilde{n}(\mathbf{k}, t) = \mathcal{F}[n(\boldsymbol{\rho}, t)]$.

The function $\frac{4\pi}{3}g_dF(\mathbf{q})$, where $\mathbf{q} \equiv \mathbf{k}l_z/\sqrt{2}$, is the k space DDI for the Q2D geometry. It has two contributions

coming from polarization perpendicular or parallel to the direction of the dipole tilt, $F(\mathbf{q}) = \cos^2(\alpha)F_\perp(\mathbf{q}) + \sin^2(\alpha)F_\parallel(\mathbf{q})$ where α is the angle between $\hat{z}$ and the polarization vector $\hat{d}$. These contributions are $F_\parallel(\mathbf{q}) = -1 + 3\sqrt{\pi}(q_d^2/q)e^{q^2}\mathrm{erfc}(q)$, where $\mathbf{q}_d$ is the wave vector along the direction of the projection of $\hat{d}$ onto the x-y plane, erfc is the complementary error function and $F_\perp(\mathbf{q}) = 2 - 3\sqrt{\pi}qe^{q^2}\mathrm{erfc}(q)$.

To simplify this problem, we rescale energies in units of the chemical potential, given by $\mu^* = gn_0\{1 + \beta\frac{4\pi}{3} \times (3\cos(\alpha)^2 - 1)\}$ for the unperturbed system [9]. Here, $\beta = g_d/g$. This leads to characteristic units of length given by the coherence length $\xi^* = \hbar/\sqrt{m\mu^*}$, time $\tau^* = \hbar/\mu^*$, and velocity $c^* = \sqrt{\mu^*/m}$. Additionally, we rescale the wave function $\psi \rightarrow \psi/\sqrt{n_0}$ where n_0 is the integrated 2D density of the unperturbed system. The rescaled coupling constants are then $g^* = gn_0/\mu^*$ and $g_d^* = g_dn_0/\mu^* = \beta g^*$.

The dispersion relation of a homogeneous Q2D DBEC is given in Bogoliubov theory by [10]

$$\omega(\mathbf{k}) = \sqrt{\frac{k^4}{4} + k^2 g^*\left(1 + \frac{4\pi}{3}\beta F\left(\frac{\mathbf{k}l_z}{\sqrt{2}}\right)\right)}. \quad (2)$$

For $\alpha = 0$ (polarization along the trap axis) this dispersion does not depend on the direction of the quasiparticle propagation. However, for $\alpha \neq 0$, or for nonzero projection of $\hat{d}$ onto the x-y plane, the direction of $\mathbf{k}$ becomes important in describing the quasiparticles of the system. The Landau critical velocity is determined from the dispersion relation via $v_L = \min[\omega(\mathbf{k})/k]$ [1] so it also depends on the direction of $\mathbf{k}$ and is an anisotropic quantity when $|\cos(\alpha)| < 1$. Other anisotropic dispersions have been predicted for a 1D lattice system of Q2D DBECs [11], periodically dressed BECs [12] and for dipolar gases in a 2D lattice [13]. Additionally in this vein, anisotropic solitons have been predicted for dipolar gases [14].

To illustrate the anisotropy in v_L, we use the parameters $g^* = 0.25$, $g_d^* = 0.36$, $l_z/\xi^* = 0.5$ and $\alpha = \pi/4$ ($\mu^* = 1$), which are chosen to best illustrate anisotropic effects while keeping safely away from the unstable regime; we will identify them with experimental parameters below. Figure 1(a) shows the dispersion calculated using these parameters for quasiparticle propagation parallel to ($\parallel$) and perpendicular to ($\perp$) the tilt of the dipoles into the plane. For parallel propagation, the dispersion resembles that of a system with contact interactions; the curve goes smoothly from the linear phonon regime at small k to the free-particle regime at large k. For this case, $v_L/c^* = 1.0$ (dashed red line), meaning that the critical velocity is identical to the speed of sound. In contrast, the perpendicular dispersion curve exhibits a rotonlike feature at intermediate k, setting $v_L/c^* = 0.50$ (dashed blue line). The inset in Fig. 1(a) shows v_L as a function of the azimuthal angle, η, the angle between $\mathbf{k}_d$ and $\mathbf{k}$. Interestingly, the speed of sound, given by
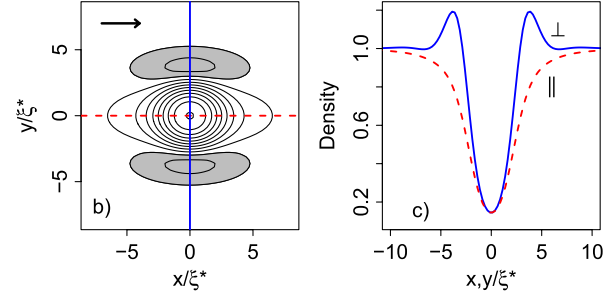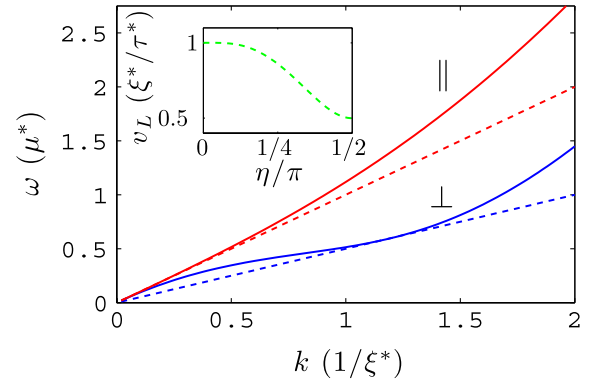

FIG. 1 (color online). (a) The Bogoliubov dispersions for $g^* = 0.25$, $g_d^* = 0.36$, $l_z/\xi^* = 0.5$ and $\alpha = \pi/4$ for propagation perpendicular ($\perp$) to and parallel ($\parallel$) to the tilt of the dipoles, shown by the blue and red lines, respectively. The dashed lines have slopes that are the Landau critical velocities (v_L) of the dispersions, while the inset shows v_L as a smooth function of the angle η between the $\parallel$ ($\eta/\pi = 0$) and $\perp$ ($\eta/\pi = 1/2$) propagation directions. (b) A contour plot of the density for a stationary obstacle with amplitude $A_p/\mu^* = 1.0$. The shaded region indicates a density exceeding $1.05n_0$, and the arrow indicates the direction of polarization. (c) Density slices of (b) along the parallel (dashed red) and perpendicular (blue) directions. The density oscillation due to the roton is clear in the perpendicular case.

$c_s = \lim_{k\to 0}[\omega(k)/k]$, is the same for both parallel and perpendicular propagation, $c_s/c^* = 1$, and is in fact isotropic. Therefore, the anisotropy in the spectrum occurs only at finite k due to the presence of an anisotropic roton.

The impact of the anisotropic roton can be directly seen in the density of the gas. In Fig. 1(b) we show a contour plot of the density in the presence of a repulsive Gaussian potential, or "probe," of the form $V_p(x, y) = A_p \exp(-(x^2 + y^2)/\sigma_p^2)$ with $A_p/\mu^* = 1.0$ and $\sigma_p/\xi^* = 2.0$, as may be realized by shining a blue-detuned laser on the system from the z direction. The shaded regions indicate density above $1.05n_0$, and the arrow indicates the direction of polarization. In Fig. 1(c) we plot density slices of this distribution to more clearly show the density profile in the parallel (dashed red) and perpendicular (solid blue) directions. Interestingly, the high-density regions occur in the direction perpendicular to the tilt of the dipoles, the same direction that exhibits a roton feature in the dispersion. Rotons have been shown to generate density modulations in perturbed DBECs [15]. Here we show this modulation can be anisotropic.

We now address the question of what happens to this anisotropic DBEC when the probe is moved through it with velocity **v**, by numerically solving Eq. (1) with the Gaussian potential $V_p(x - vt, y)$. For concreteness, we consider motion parallel and perpendicular to the tilt of the dipoles by tilting $\hat{d}$ into the $\hat{x}$ and $\hat{y}$ directions, respectively, while fixing the direction of the probe velocity so that $\mathbf{v} = v\hat{x}$.

Figure 2(a) shows the time-averaged drag force (averaged up to $t = 100\tau^*$) acting on a "weak" probe with parameters $A_p/\mu^* = 0.1$ and $\sigma_p/\xi^* = 2.0$. The force at time t is given by $\mathbf{F}(t) = -\int d^2\rho |\psi(\boldsymbol{\rho}, t)|^2 \vec{\nabla} V_p(\boldsymbol{\rho}, t)$ [16]. In this case, the probe is sufficiently weak so that no vortices are nucleated in the fluid, and instead only quasiparticles are excited. The presence of a force on the probe signifies the excitation of quasiparticles, and thus the breakdown of superfluid flow. There is a clear anisotropic onset of force in these simulations that agrees very well with the anisotropic v_L given by the Bogoliubov dispersions in Fig. 1(a), resulting in critical velocities of $v_c/c^* = 0.90(0.46)$ for parallel (perpendicular) motion of this probe, determined by the velocity at which the drag force suddenly rises.

It has been shown that v_L is recovered as the true critical velocity only when the superfluid is perturbed by a vanishingly small object [17,18]. Additionally, while quasiparticle excitations are a natural feature to study when considering the breakdown of superfluid flow, they may be difficult to observe experimentally. Vortices, on the other hand, are superfluid excitations in the form of topological defects that create regions of zero density and are easier to observe experimentally than quasiparticles. The first measurements of v_c in a BEC were from observations of the sudden onset of heating [7,8], believed to be related to vortex production in the BECs. More recently, Ref. [19] used experimental finesse to controllably create vortex pairs to observe v_c. Motivated by these circumstances, we investigate the critical velocity for vortex formation in the Q2D DBEC by using a moving probe with an amplitude that is linearly ramped from $A_p = 0$ to $A_p/\mu^* = 1.0$ in a time $10\tau^*$ with $\sigma_p/\xi^* = 2.0$. The critical velocity in this case corresponds to the probe velocity above which vortices are formed, signaling the breakdown of superfluidity.

We observe a significant difference in the critical velocity at which vortices are formed between a probe moving parallel and perpendicular to the dipole polarization. In Fig. 2(b) we show the maximum number of vortices formed within $t/\tau^* = 100$. The critical velocities are $v_c = 0.46(0.28)$ for motion parallel (perpendicular) to the dipole tilt. These values are about half the value of the critical velocities obtained using the weaker probe, but this is not unexpected [16,20]. In a superfluid, vortices have quantized circulation: $\oint \mathbf{v} \cdot d\mathbf{l} = 2\pi\hbar n/m$, where **v** is the velocity field of the fluid and n is an integer, corresponding to phase winding of $2\pi n$ around the vortex core. We count vortices in our simulations by finding the phase winding on a plaquette of grid points [21].
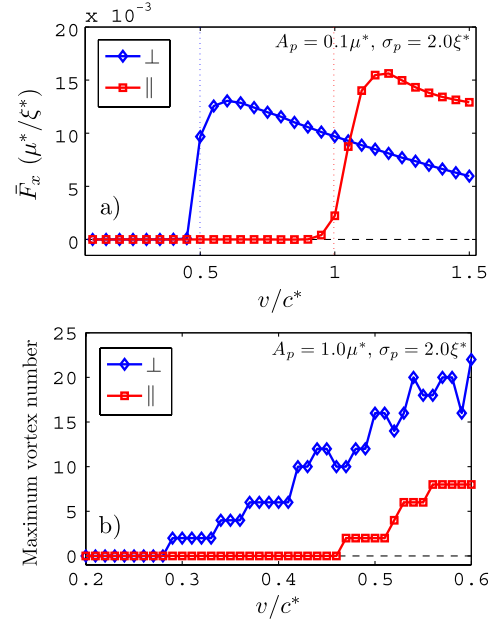

FIG. 2 (color online).   (a) The mean drag force acting on the probe with $A_p/\mu^* = 0.1$ and $\sigma_p/\xi^* = 2.0$ calculated up to time $t/\tau^* = 100$ for motion perpendicular to (blue diamonds) and parallel to (red squares) the dipole tilt. The dotted lines represent the corresponding v_L, in excellent agreement with the numerical simulations. (b) The maximum vortex number produced by a probe with $A_p/\mu^* = 1.0$ and $\sigma_p/\xi^* = 2.0$ calculated up to $t/\tau^* = 100$ for motion perpendicular to (blue diamonds) and parallel to (red squares) the dipole tilt. The corresponding critical velocities are: $v_c^{(\perp)}/c^* = 0.27$ and $v_c^{(\parallel)}/c^* = 0.46$.

The physical mechanism that sets the critical velocity for vortex formation is not rigorously understood. However, it is theorized that the maximum local fluid velocity about an obstacle, being larger than the background flow velocity, sets the critical velocity via the Landau criterion. This idea has been fruitful [16,20], and we find qualitative agreement with this theory here, as the direction with lower v_c is also the direction of flow most likely to spawn vortices. However, we note that the DDI is anisotropic although the fully condensed (ground) state of the system is completely isotropic. The anisotropies only appear in the dispersion relation and in the ground state of the system in the presence of a perturbing potential, which is intimately related to the dispersion relation [15]. Thus, the anisotropies in the critical velocity for vortex formation are due to the anisotropy of the roton mode, just like the critical velocities for quasiparticle excitations.

Figure 3 shows contour plots of the condensate density for both parallel (red contours, top row) and perpendicular (blue contours, bottom row) motion of the probe relative to the dipole tilt for velocities $v/c^* = 0.3$ (left column) and $v/c^* = 0.5$ (right column), where the probe is moving in the $\hat{x}$ direction and is located at the origin at the time shown in Fig. 3. Recall that $v/c^* = 0.3$ is just above v_c for vortex formation for perpendicular motion, but well beneath v_c for parallel motion. This is reflected in the figure, where in
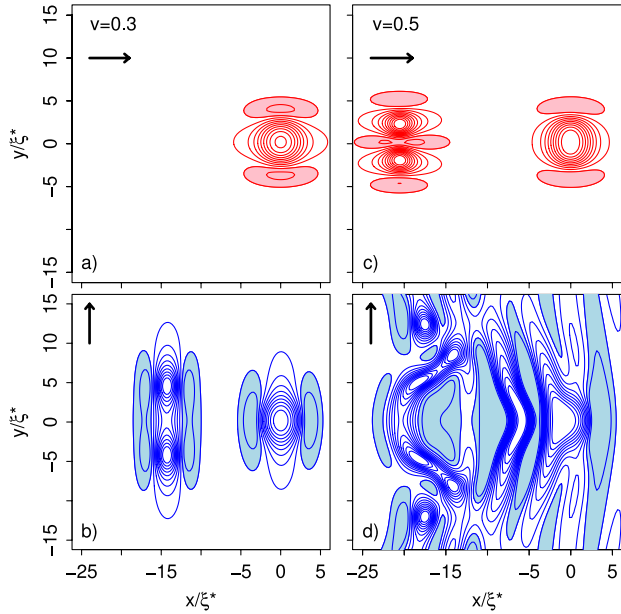
FIG. 3 (color online). (a) and (b) The densities are shown for the $\parallel$ (top, red) and $\perp$ (bottom, blue) cases for $v/c^* = 0.30$ and $t/\tau^* = 125$. Only the $\perp$ case has exceeded its v_c. (c) and (d) Densities for $v/c^* = 0.50$ at $t/\tau^* = 100$. The parallel case (top, red) has exceeded its critical velocity and the perpendicular case (bottom, blue) has been wildly excited. The obstacle is at $x = y = 0$ and moving in the $+x$ direction. The shaded regions of this plot occur when the density exceeds $1.05 n_0$, and the arrows indicate the direction of dipole tilt.

(a) no vortices have been formed for parallel motion, while in (b) a vortex pair has been formed for perpendicular motion for the same probe velocity.

For the case of $v/c^* = 0.5$, we see that the parallel case in (c) has formed a vortex pair, and in (d) the perpendicular case has been wildly excited. There is an important contrast to be made in the density profiles when there is a single vortex pair in (b) and (c). In the parallel case (c) we see that a *high* density region occurs between the vortex pair and is elongated in the polarization direction. In contrast, for the perpendicular case (b) there is a low density region between the vortex pair and high-density regions on either side of the vortex pair. Both the anisotropic superfluid critical velocity for vortex pair production and these contrasting density profiles present means to observe the effects of the roton in DBEC directly.

In addition to investigating this Q2D system, we have performed simulations for a fully trapped DBEC. For a trap aspect ratio of $\lambda = \omega_z/\omega_\rho = 50$, we find that critical velocities for vortex production are strongly anisotropic, and the v_c are numerically similar to the free case. In these simulations, we start the probe in the center of the trap and move outwards in the parallel or perpendicular direction, linearly ramping the amplitude of the laser down to zero by the time it reaches the zero density region. Such a simulation is experimentally realizable in a DBEC of atomic ^{52}Cr, for example, having a permanent magnetic

dipole moment of $6\mu_B$ where μ_B is the Bohr magneton, for a DBEC with particle number $N \simeq 18.5 \times 10^3$, scattering length $a_s = 5.0a_0$ where a_0 is the Bohr radius, radial trap frequency $\omega_\rho = 2\pi \times 20$ Hz and a blue-detuned laser with width $\sigma_p = 1.76$ μm. The speed of sound in this system is $c_s = 0.16$ cm/s in the center of the trap.

In conclusion, we have characterized the DBEC as an anisotropic superfluid by performing numerical simulations of a blue-detuned laser moving through the system in directions parallel and perpendicular to the dipole polarization. We find a sudden onset of drag on the laser at velocities that depend strongly on the direction of motion, and attribute the anisotropy in critical velocity to the anisotropic roton so that a measurement of an anisotropic critical velocity in a DBEC corresponds to a measurement of the roton in the system. Additionally, by considering a DBEC that is experimentally realizable with atomic ^{52}Cr, we propose a single, stable constituent with which to study anisotropic superfluidity, while other systems such as superfluids of d-wave Cooper pairs are more conceptually and experimentally difficult to control.

[1] L. D. Landau, J. Phys. (Moscow) **5**, 71 (1941).
[2] D. R. Allum *et al.*, Phil. Trans. R. Soc. A **284**, 179 (1977).
[3] Th. Lahaye *et al.*, Nature (London) **448**, 672 (2007); Th. Lahaye *et al.*, Phys. Rev. Lett. **101**, 080401 (2008).
[4] L. D. Carr *et al.*, New J. Phys. **11**, 055049 (2009).
[5] L. Santos *et al.*, Phys. Rev. Lett. **90**, 250203 (2003).
[6] R. M. Wilson, S. Ronen, and J. L. Bohn, Phys. Rev. Lett. **104**, 094501 (2010).
[7] C. Raman *et al.*, Phys. Rev. Lett. **83**, 2502 (1999).
[8] R. Onofrio *et al.*, Phys. Rev. Lett. **85**, 2228 (2000).
[9] R. Nath, P. Pedri, and L. Santos, Phys. Rev. Lett. **102**, 050401 (2009).
[10] U. R. Fischer, Phys. Rev. A **73**, 031602(R) (2006).
[11] D. W. Wang and E. Demler, arXiv:0812.1838v1.
[12] J. Higbie and D. M. Stamper-Kurn, Phys. Rev. Lett. **88**, 090401 (2002).
[13] I. Danshita and D. Yamamoto, Phys. Rev. A **82**, 013645 (2010).
[14] I. Tikhonenkov, B. A. Malomed, and A. Vardi, Phys. Rev. Lett. **100**, 090406 (2008).
[15] R. M. Wilson *et al.*, Phys. Rev. Lett. **100**, 245302 (2008).
[16] T. Winiecki *et al.*, J. Phys. B **33**, 4069 (2000).
[17] J. S. Steißberger and W. Zwerger, Phys. Rev. A **62**, 061601 (R) (2000).
[18] S. Ianeselli *et al.*, J. Phys. B **39**, S135 (2006).
[19] T. W. Neely *et al.*, Phys. Rev. Lett. **104**, 160401 (2010).
[20] T. Frisch, Y. Pomeau, and S. Rica, Phys. Rev. Lett. **69**, 1644 (1992).
[21] C. Foster *et al.*, Phys. Rev. A **81**, 023623 (2010).